

# Modelling the moisture effect on the rate of spread of fire in a leaf-like fuel element

**Author:**

Edalati-nejad, Ali; Ghodrat, Maryam; Sharples, Jason J

**Publication details:**

2653-0597 (ISSN)

**Event details:**

23rd Australasian Fluid Mechanics Conference – 23AFMC

Sydney

2022-12-04 - 2022-12-08

**Publication Date:**

2022-12-22

**DOI:**

<https://doi.org/10.26190/unsworks/28593>

**License:**

<https://creativecommons.org/licenses/by/4.0/>

Link to license to see what you are allowed to do with this resource.

Downloaded from [http://hdl.handle.net/1959.4/unsworks\\_83463](http://hdl.handle.net/1959.4/unsworks_83463) in <https://unsworks.unsw.edu.au> on 2024-05-18

# Modelling the moisture effect on the rate of spread of fire in a leaf-like fuel element

Ali Edalati-nejad<sup>1</sup>, Maryam Ghodrat<sup>2\*</sup> and Jason J. Sharples<sup>1\*</sup>

<sup>1</sup> School of Science, UNSW Canberra, Canberra, ACT 2612, Australia

<sup>2</sup> School of Engineering and Information Technology, UNSW Canberra, Canberra, ACT 2612, Australia

\* Email: [j.sharples@adfa.edu.au](mailto:j.sharples@adfa.edu.au), [m.ghodrat@unsw.edu.au](mailto:m.ghodrat@unsw.edu.au)

## Abstract

In this study, the effect of fuel moisture content (FMC) on the pyrolysis, ignition, and rate of drying processes of a leaf-like fuel element is numerically investigated. To start the ignition, an upward hot airflow is placed under the leaf-like fuel source. The dry fuel was considered as cellulose. The current study is validated against published experimental data, using the time history of fuel mass loss measurement. The effect of FMC on the mass fraction of oxygen is also investigated. The transient solver of FireFOAM, which uses the Large Eddy Simulation (LES), is used to perform the numerical simulations. The results confirm that an increase in the amount of fuel moisture content leads to a decrease in the rate of spread of the fire and an increase in the drying process time.

It is also found that during both drying and pyrolysis process, different parts of a selected fuel element have different temperatures. This is mainly due to the decrease of moisture concentration near the ignition point. Results showed that at  $t = 6.5$  s the volumetric average temperature of the solid fuel for the case with FMC 26%, is 642 K while for FMC of 34%, this temperature is 605 K.

## 1. Introduction

Wildfires may result in environmental disasters, and economic damages, including damages to properties, emission of pollutions, and can trigger climate change by flooding, erosions, and debris flows (Verma, 2019). Wildfires are also important elements of ecosystem management and functional ecosystems, despite the fact that they may result in major economic and ecological damages (Menage et al., 2012).

To tackle and manage the abovementioned problems, people interact with wildfires in various ways such as setting prescribed fires to reduce their damage (Canfield et al., 2014). Population growth and higher demand for living closer to forested areas, have made it more crucial to further develop our understanding of wildfire behaviour and to enhance our ability in predicting fire dynamic characteristics in different geographical and atmospheric conditions.

Despite years of investigation in the domain of fire science, current knowledge of wildfire behaviour is still very limited (Finney et al., 2012) due to the variety of complicated physical and chemical reactions and interactions associated with this natural hazard (Verma, 2019).

The key factor in understanding wildfire hazards and finding the most practical way to deal with them is to be able to accurately predict the complex physics of the problem including the interaction and coupling of the driving processes (wind, buoyancy induced flow, combustion, thermal radiation, thermal degradation of vegetation, etc.). Furthermore, important factors such as topographic and atmospheric conditions, fuel structure and fuel moisture content (FMC) play critical roles in determining the dominant behaviour of wildfires (Verma, 2019).

These factors have been examined extensively in the literature, for example: topographic and atmospheric conditions have been examined by Edalati-nejad et al. (2021), Sharples et al. (2018), Sullivan et al. (2014), Verma (2019); fuel structure effects, including fire intensity have been examined by Clark et al. (2020), Edalati-nejad et al. (2022), Frangieh et al. (2020), Fryanova and



Perminov (2017); and fuel moisture content (FMC) by Moinuddin et al. (2021), Morvan (2013), and Yashwanth et al. (2016).

Fuel moisture, for instance, has a big impact on the ignition, pyrolysis process, and rate of spread of wildland fires (Weise & Wright, 2014). Yashwant et al. (2014) conducted a numerical study on the effect of moisture content on pyrolysis and combustion of live fuels. Live fuels were examined with moisture content varying from 30 to 200%. The chosen fuel was thin cellulosic material with a dimension of a typical Manzanita (*Arctostaphylos glandulosa*) leaf that was exposed to a radiant heat source. Their findings showed that the case with lower moisture content was ignited earlier in time and resulted in higher solid and gas phase temperatures. Moinuddin et al. (2021) investigated the effect of relative humidity and fuel moisture content on grassfire propagation. Four sets of grassfire simulations were examined. Their results indicated that fuels with lower (FMC) were associated with higher fire intensity and rate of spread values.

The effect of moisture content on autoignition and thermal decomposition of wood was studied by Gong et al. (2020). Beech wood was considered as solid fuel, with fuel moisture contents ranging from 0% to 38%. It was shown that the in-depth and surface temperatures increased more rapidly with higher values of heat flux and lower fuel moisture contents. Also, the ignition time increased in response to increasing fuel moisture content. In another investigation, fire behaviour in leaves and sparse shrubs was experimentally studied and modelled (Prince, 2014). In this work a model based on convective heat transfer of fire spread in shrubs was developed based on experimental measurements. The authors selected four different groups of dry dead leaves, rehydrated dead leaves, dehydrated live leaves, and fresh live leaves with 4, 26, 34, and 63% fuel moisture content, respectively. Results revealed that the dead leaves released pyrolysis gas much faster than the live fuels.

Borujerdi et al. (2020) conducted a numerical study of burning of leaves with different fuel moisture contents exposed to a convective heat source. In their study, ignition, combustion, and pyrolysis of a solid fuel of manzanita were numerically investigated. Looking at the time history of heat release rate, it was reported that an increase in fuel moisture content leads to a delay in the ignition time. It was also shown that a significant amount of moisture remained in the leaf after the ignition.

The aforementioned investigations have expanded knowledge of the effect of fuel moisture content on ignition and pyrolysis processes. However, less attention has been paid to the role of rate of pyrolysis and drying process of a solid fuel on fire propagation. Wildfires involve the ignition and burning of many solid fuel elements, including leaves, twigs and branches, and so understanding how the burning of individual solid fuel elements, such as thin cellulosic leaves, is affected by fuel moisture content can provide detailed insights into how wildfires burn. The objective of this study, therefore, is to numerically investigate the effect of moisture content on the rate of pyrolysis, fire spread and drying process for a solid fuel exposed to a convective heat source, at two different fuel moisture contents of rehydrated dead (26%), and dehydrated live (34%).

## 2. Physical model

In this study, a cellulose leaf (Yashwanth et al., 2016) is considered as a solid fuel with two different fuel moisture contents, exposed to a convective heat source, which generates hot gases with a constant velocity. The computational domain, which has dimensions of 0.18 m (x) × 0.25 m (y) × 0.32 m (z) is shown in Figure 1. A solid fuel leaf is placed in the centre of the computational domain, 0.04 m above the bottom surface of the domain, with dimensions of 23.7 mm × 0.51 mm × 23.7 mm.

A structured mesh with a high-resolution area in the vicinity of the leaf and near the convective heat source, is used. The convective heat source enters 10 mol% O<sub>2</sub> at 1273K and 0.6 m/s, similar to the experimental conditions of (Prince, 2014).

To simulate the chemical combustion reaction of pyrolysis gases, a single step reaction of air/methane is used and showed in eq. 1. This is because the main gas products from the pyrolysis of vegetative fuels are CO<sub>2</sub>, CO, and CH<sub>4</sub> (Dahale et al., 2013; Yang et al., 2007).

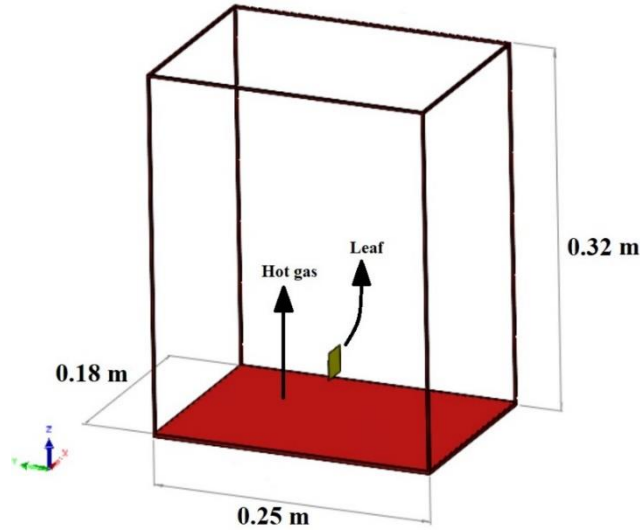
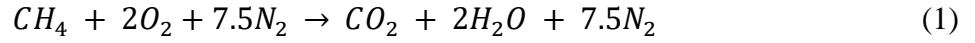


Figure 1. Schematic of the computational domain.

### 3. Mathematical and reaction models

In the current study, to solve the governing equations, an open-source solver of OpenFOAM namely FireFOAM, is used. FireFOAM is a practical and useful tool to simulate fire dynamic behaviour and pyrolysis reactions (Le et al., 2018). FireFOAM also benefits from having several CFD sub-models to simulate fire dynamic problems such as radiant and convective heating effects, pyrolysis, and turbulent and laminar combustion.

In the present study, the Reynolds number, at the inlet of the domain is 1100, which is in the range of laminar flame. After the ignition, the combustion leads to have the turbulent flow, at the downstream above the leaf solid fuel. in order to obtain the effects of turbulent flow on the fire behaviour, at the vicinity of the flame and to capture vorticity effects near the combustion area, the Large Eddy Simulation (LES) (Wang et al., 2011) turbulence model is used. This is because combustion results in an intense change in local temperature and pressure, which produces local vorticity and movement in the flow, which results in localised turbulence. Also, the wall-adapting local eddy (WALE)-viscosity method (Ren et al., 2013) is employed as it has been designed for large-eddy simulation (LES) of a turbulent boundary layer, in transitional flow and it can correctly capture the asymptotic decay of the eddy viscosity in the vicinity of a solid wall in the turbulent boundary layer (Kim et al., 2020). Considering a single step combustion reaction of methane, the combustion model of infinitely fast chemistry (Mahle et al., 2006) is applied. In this simulation, only the condensed phase of moisture is considered (Gong et al., 2020). The governing equations for the pyrolysis and vaporisation are as follows (Ding et al., 2015):

$$\frac{\partial(\rho_s Y_{cellulose})}{\partial t} = \dot{\omega}_{cellulose}, \quad (2)$$

$$\frac{\partial(\rho_s Y_{moisture})}{\partial t} = \dot{\omega}_{moisture}, \quad (3)$$

$$\dot{\omega}_{wood} = \left[ \frac{\rho_s Y_{cellulose}}{(\rho_s Y_{cellulose})_0} \right]^n (\rho_s Y_{cellulose})_0 A_{cellulose} \exp\left(-\frac{E_{a,cellulose}}{RT}\right), \quad (4)$$

$$\dot{\omega}_{moisture} = \left[ \frac{\rho_s Y_{moisture}}{(\rho_s Y_{moisture})_0} \right]^n (\rho_s Y_{moisture})_0 A_{moisture} \exp\left(-\frac{E_{a,moisture}}{RT}\right), \quad (5)$$

where  $E_a$  and  $A$  represent the pre-exponential factor and activation energy, respectively.  $Y$  is the mass fraction of the species of cellulose and moisture,  $\dot{\omega}$  is the mass consumption rate,  $T$  and  $\rho_s$

are temperature and averaged density of the species, respectively. The parameter  $n$  is the reaction order,  $R$  is the universal gas constant, and the subscript 0 denotes initial conditions.

The governing equations in the fluid region are as follows (Favre, 1983):

$$\frac{\partial \bar{\rho}}{\partial t} + \frac{\partial(\bar{\rho}\tilde{u}_i)}{\partial x_i} \quad (6)$$

$$\frac{\partial(\bar{\rho}\tilde{u}_i)}{\partial t} + \frac{\partial(\bar{\rho}\tilde{u}_i\tilde{u}_j)}{\partial x_j} = \frac{\partial}{\partial x_j} \left[ \bar{\rho}(v + v_t) \left( \frac{\partial(\tilde{u}_i)}{\partial x_j} + \frac{\partial(\tilde{u}_j)}{\partial x_i} - \frac{2}{3} \frac{\partial(\tilde{u}_k)}{\partial x_k} \delta_{ij} \right) \right] - \frac{\partial(\bar{P})}{\partial x_i} + \bar{\rho} g_i \quad (7)$$

$$\frac{\partial(\bar{\rho}\tilde{h})}{\partial t} + \frac{\partial(\bar{\rho}\tilde{u}_j\tilde{h})}{\partial x_j} = \frac{D\bar{P}}{Dt} + \frac{\partial}{\partial x_j} \left[ \bar{\rho} \left( \alpha_t + \frac{v_t}{Pr_t} \right) \left( \frac{\partial\tilde{h}}{\partial x_j} \right) \right] + \dot{q}''' - \nabla \cdot \dot{q}_r'' \quad (8)$$

$$\frac{\partial(\bar{\rho}\tilde{Y}_m)}{\partial t} + \frac{\partial(\bar{\rho}\tilde{u}_j\tilde{Y}_m)}{\partial x_j} = \frac{\partial}{\partial x_j} \left[ \bar{\rho} \left( D_c + \frac{v_t}{Sc_t} \right) \frac{\partial(\tilde{Y}_m)}{\partial x_j} \right] + \bar{\omega}_m \quad (9)$$

$$\bar{P} = \bar{\rho}R\tilde{T} \quad (10)$$

where  $h$  is the total enthalpy, “ $\sim$ ” and “ $\bar{\phantom{x}}$ ” denote Favre filtering and spatial averaging, respectively,  $Y_m$  is the mass fraction of species  $m$ ,  $g$  is the gravitational acceleration, and  $P$  represents the static pressure,  $\delta$ ,  $\rho$ ,  $Pr_t$ ,  $v$ ,  $D_c$ ,  $v_t$ ,  $\alpha_t$ ,  $R$ ,  $Sc_t$ , and  $\omega_m$  are Kronecker delta, density, the turbulent Prandtl number, the laminar viscosity, the laminar diffusion coefficient, the turbulent viscosity, thermal diffusion coefficient, gas constant, the turbulent Schmidt number, and production/sink rate of species  $m$  due to gas reaction, respectively. The reaction rate is calculated by the Arrhenius equation:

$$k = Ae^{\frac{-E_a}{RT}} \quad (11)$$

where  $k$  is the reaction rate,  $A$  is the pre-exponential factor,  $E_a$  is activation energy,  $R$  is universal gas constant,  $T$  is temperature, and  $\Delta Hr$  is the enthalpy of the reaction.

The reactions and kinetic parameters used in the present model is listed in Table 1.

Reaction	A (s <sup>-1</sup> )	E <sub>a</sub> (J mol <sup>-1</sup> )	Reaction order	ΔHr (J g <sup>-1</sup> )
Moisture → Vapor	5.13×10 <sup>10</sup>	8.8×10 <sup>4</sup>	1	-2.44×10 <sup>3</sup>
Cellulose → Char + Pyrolysate	7.83×10 <sup>10</sup>	1.27×10 <sup>5</sup>	4.86	-1.41×10 <sup>3</sup>

Table 1. Reactions and kinetic parameters for pyrolysis and moisture evaporation (Chaos et al., 2011).

To study the mesh dependency of the results, the domain was rendered using three different grid numbers of 324,000, 554,000, and 736,000, and the results of the respective simulations were compared. Increasing the mesh number from 324,000 to 554,000 resulted in a considerable change in the normalized mass of the solid fuel, but a further increase to 736,000 had less of an effect on the result. As such, the mesh number of 554,000 was selected for all subsequent simulations, as a compromise to limit computational costs.

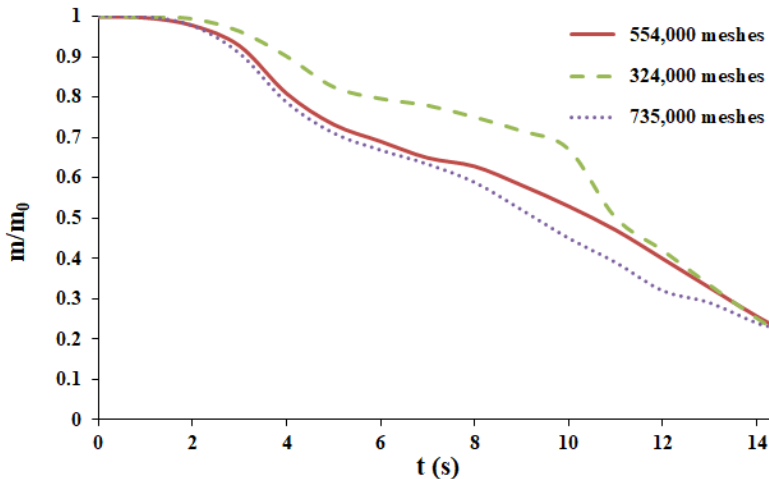


Figure 2. Comparison between the normalized mass for three different grid numbers.

To validate the simulations, the time history diagram of the normalized mass of the leaf, with a fuel moisture content of 34%, is shown in Figure 3. The figure shows the numerical results of the present study, along with the experimental measurements of Prince (2014). The figure indicates an acceptable level of agreement between the numerical and experimental results. More specifically, good agreement is found during the early stages of burning followed by a moderate divergence of the results after about  $t = 6$  s. The maximum discrepancy is about 10% and occurs at about  $t = 11$  s. The discrepancy between the simulated data and experimental measurements could be partly related to the solid fuel pyrolysis kinetic model, because in a real scenario, the solid fuel may contain small amounts of protein and lipid (Matt, F. J., Dietenberger, M. A., & Weise, D. R., 2020).

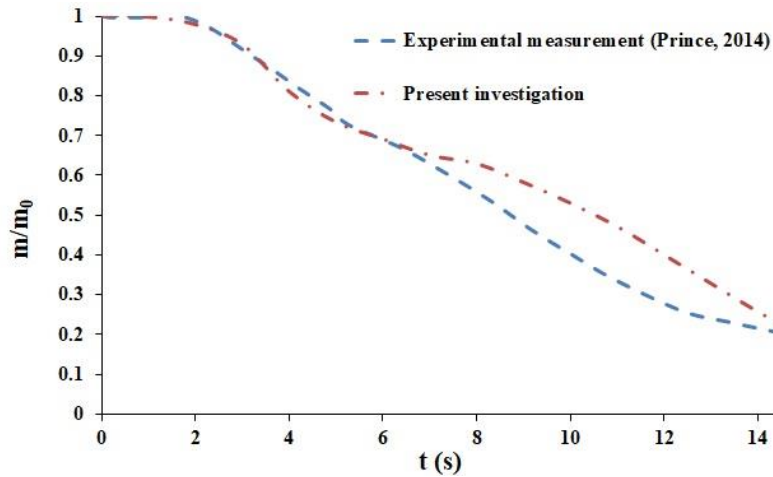


Figure 3. Time history diagram of the normalized mass of the solid fuel for the present study and experimental data (Prince, 2014) for the case with the fuel moisture content of 34%.

#### 4. Results

The time history diagram of the normalized moisture mass is shown in Figure 4. As can be seen, the rate of drying for the case with  $FMC = 26\%$  is higher than the case with  $FMC = 34\%$ . This is due to the fact that the case with lower FMC heats up more than that of with higher FMC, which is associated with having a higher radiative absorption coefficient.

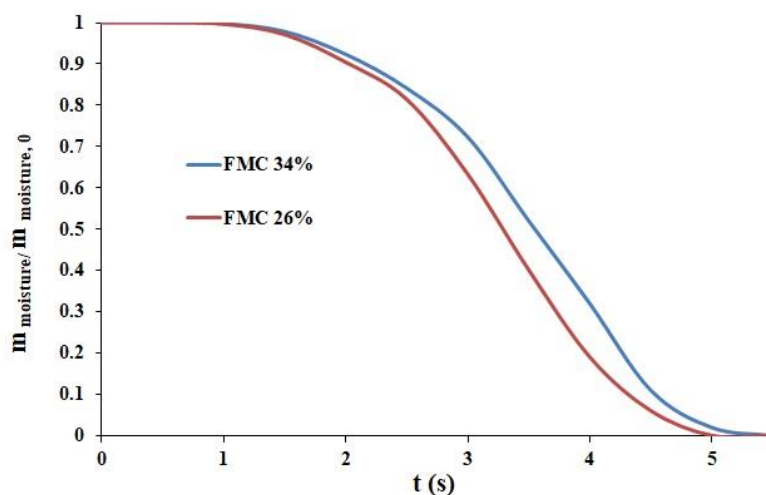


Figure 4. Time history diagram of the normalized moisture mass for two different cases with  $FMC = 34\%$  and  $FMC = 26\%$ .

The temperature within the domain at the moment of ignition for two cases of  $FMC = 26\%$ , and  $34\%$  are shown in Fig. 5. The threshold temperature in the domain for the ignition is assumed to be 1700 K. As there were no combustion in the time before, the shown frames have been determined as the

ignition time. As seen, the case with 26% FMC, ignited at 2.4s, and the case with 34%, start ignition at 2.65s. At this moment, the maximum temperature of the solid fuel, itself, is 950K, which can be considered as the ignition temperature for the solid fuel.

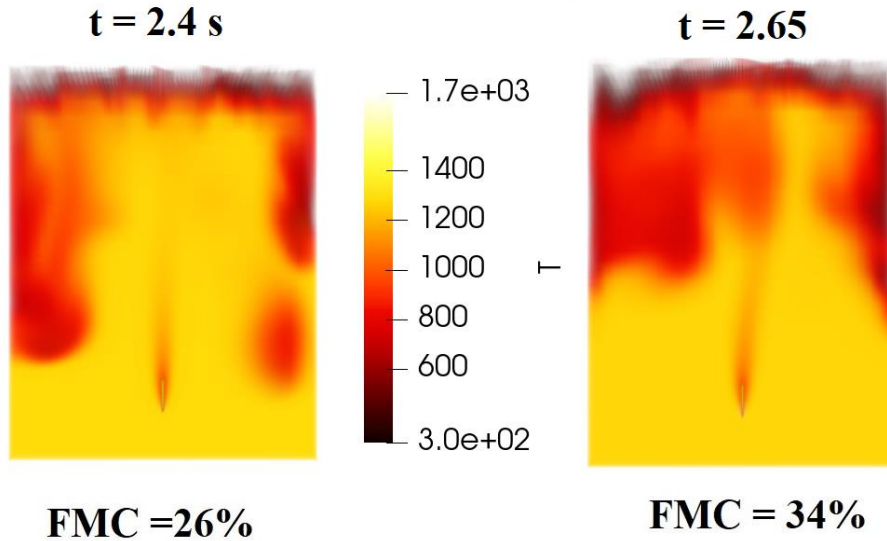


Figure 5. Temperature in the domain at the moment of ignition for two fuel moisture contents of 26%, and 34%.

Temperature distributions of the leaf-like solid fuel at different times of 2.5, 4.5, and 6.5 s, and for the two FMCs of 26 and 34% are shown in Figure 6. As is evident from the figure, the temperature of the cases with lower FMC increases more rapidly, such that after 6.5 seconds the volumetric average temperature of the solid fuel for the case with lower FMC (26%), is higher (624 K) while, the volumetric average temperature is lower (605 K) for the case with higher fuel moisture content (34%). The temperature distributions can also be used to infer the rate of fire spread in the solid fuel so it can be found from both figures 4 and 5 that in the case with lower fuel moisture content, the rate of drying process and increasing temperature is higher than the case with higher amount of FMC.

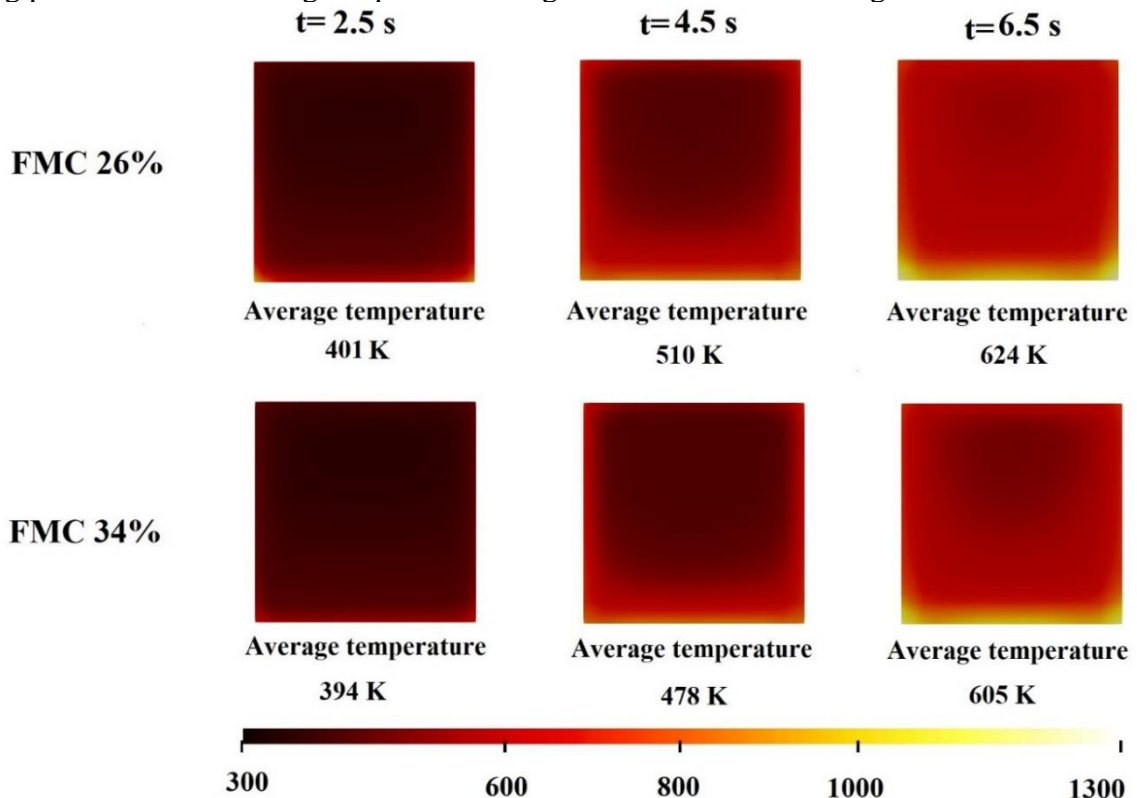


Figure 6. Temperature distribution in the solid fuel at different times and for two fuel moisture contents of 26%, and 34%.

Cross sections ( $x=0$ ) of oxygen concentration at  $t=3$  s, for both cases of 26%, and 34% FMCs are shown in Figure 7. As is evident from these cross sections, the case with lower FMC has the lowest amount of oxygen at the vicinity of the solid fuel, which indicates that ignition is occurring at  $t=3$  s. On the other hand, for the case with higher fuel moisture content (34%), ignition has not yet completely occurred at  $t=3$  s.

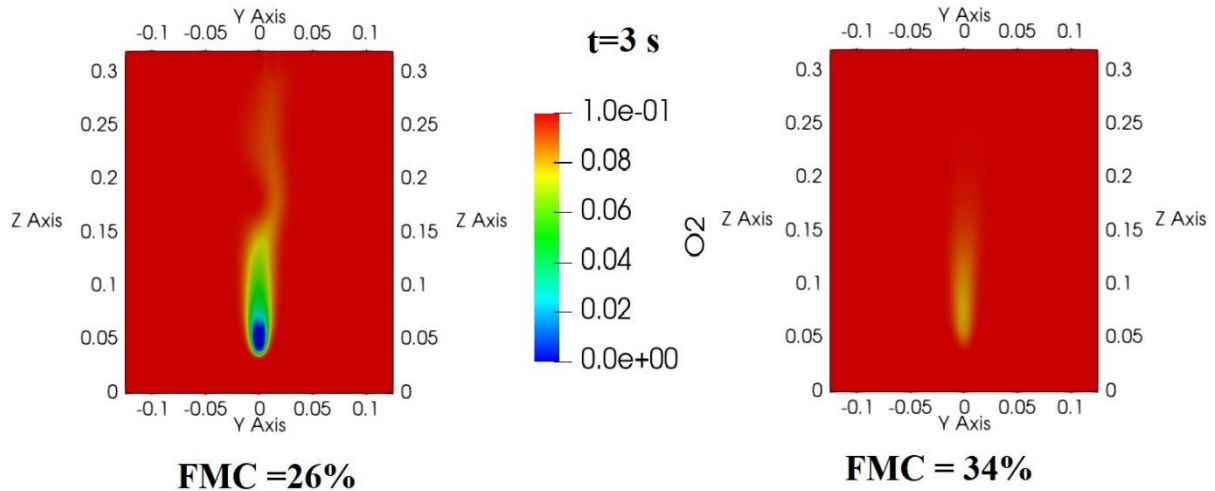


Figure 7. Cross sections of Oxygen mass fraction distribution for the cross section of the domain, for two different fuel moisture contents of 26, and 34%.

The FMC has a significant relation with the ignition process which influences fire formation. The current study helps to understand how the solid fuel ignites and its relationship with factors such as moisture content.

## 5. Conclusions

In the present investigation, the effect of moisture content on the rate of pyrolysis, and drying process for a leaf-like solid fuel, exposed to a convective heat source of 1273 K, for two different fuel moisture contents of 26, and 34% is studied. The main results of the present investigation are summarized as follows:

- The computational results have an acceptable agreement with the experimental measurements (in the absence of fuel moisture).
- The rate of drying of the leaf-like solid fuel with FMC of 26% is higher than the case with FMC of 34%. This is due to the higher radiative absorption coefficient associated with the lower FMC case
- At  $t= 6.5$  s the volumetric average temperature of the solid fuel for the case with a FMC of 26%, is 624 K while for the case with a higher FMC of 34% it is 605K.

## Acknowledgments

The current work was conducted with the assistance of resources provided by the National Computational Infrastructure (NCI) National Facility at the Australian National University through the National Computational Merit Allocation Scheme supported by the Australian Government.

This work is also supported by a PhD Scholarship from the University of New South Wales.

## References

Borujerdi, P. R., Shotorban, B., & Mahalingam, S. (2020). A computational study of burning of vertically oriented leaves with various fuel moisture contents by upward convective heating. *Fuel*, 276, 118030.



- Canfield, J., Linn, R., Sauer, J., Finney, M., & Forthofer, J. (2014). A numerical investigation of the interplay between fireline length, geometry, and rate of spread. *Agricultural and Forest Meteorology*, 189, 48-59.
- Chaos, M., Khan, M. M., Krishnamoorthy, N., de Ris, J. L., & Dorofeev, S. B. (2011). Evaluation of optimization schemes and determination of solid fuel properties for CFD fire models using bench-scale pyrolysis tests. *Proceedings of the Combustion Institute*, 33(2), 2599-2606.
- Clark, K. L., Heilman, W. E., Skowronski, N. S., Gallagher, M. R., Mueller, E., Hadden, R. M., & Simeoni, A. (2020). Fire behavior, fuel consumption, and turbulence and energy exchange during prescribed fires in pitch pine forests. *Atmosphere*, 11(3), 242.
- Dahale, A., Ferguson, S., Shotorban, B., & Mahalingam, S. (2013). Effects of distribution of bulk density and moisture content on shrub fires. *International journal of wildland fire*, 22(5), 625-641.
- Ding, Y., Wang, C., & Lu, S. (2015). Modeling the pyrolysis of wet wood using FireFOAM. *Energy conversion and management*, 98, 500-506.
- Edalati-nejad, A., Ghodrat, M., Fanaee, S. A., & Simeoni, A. (2022). Numerical Simulation of the Effect of Fire Intensity on Wind Driven Surface Fire and Its Impact on an Idealized Building. *Fire*, 5(1), 17.
- Edalati-nejad, A., Ghodrat, M., & Simeoni, A. (2021). Numerical investigation of the effect of sloped terrain on wind-driven surface fire and its impact on idealized structures. *Fire*, 4(4), 94.
- Favre, A. (1983). Turbulence: Space-time statistical properties and behavior in supersonic flows. *The Physics of fluids*, 26(10), 2851-2863.
- Finney, M. A., Cohen, J. D., McAllister, S. S., & Jolly, W. M. (2012). On the need for a theory of wildland fire spread. *International journal of wildland fire*, 22(1), 25-36.
- Frangieh, N., Accary, G., Morvan, D., Méradji, S., & Bessonov, O. (2020). Wildfires front dynamics: 3D structures and intensity at small and large scales. *Combustion and flame*, 211, 54-67.
- Fryanova, K., & Perminov, V. (2017). Impact of forest fires on buildings and structures. *Magazine of Civil Engineering*(7(75)), 15-22.
- Gong, J., Cao, J., Zhai, C., & Wang, Z. (2020). Effect of moisture content on thermal decomposition and autoignition of wood under power-law thermal radiation. *Applied Thermal Engineering*, 179, 115651.
- Kim, M., Lim, J., Kim, S., Jee, S., & Park, D. (2020). Assessment of the wall-adapting local eddy-viscosity model in transitional boundary layer. *Computer Methods in Applied Mechanics and Engineering*, 371, 113287.
- Le, D., Labahn, J., Beji, T., Devaud, C. B., Weckman, E. J., & Bounagui, A. (2018). Assessment of the capabilities of FireFOAM to model large-scale fires in a well-confined and mechanically ventilated multi-compartment structure. *Journal of fire sciences*, 36(1), 3-29.
- Mahle, I., Mellado, J., Sesterhenn, J., Friedrich, R., & de Ingenieros, S. (2006). LES of reacting turbulent shear layers using infinitely fast chemistry. *Contribution to: Turbulence and Interaction*.
- Menage, D., Chetehouna, K., & Mell, W. (2012). Numerical simulations of fire spread in a Pinus pinaster needles fuel bed. *Journal of Physics: Conference Series*,
- Moinuddin, K., Khan, N., & Sutherland, D. (2021). Numerical study on effect of relative humidity (and fuel moisture) on modes of grassfire propagation. *Fire Safety Journal*, 125, 103422.
- Morvan, D. (2013). Numerical study of the effect of fuel moisture content (FMC) upon the propagation of a surface fire on a flat terrain. *Fire Safety Journal*, 58, 121-131.
- Prince, D. R. (2014). *Measurement and modeling of fire behavior in leaves and sparse shrubs*. Brigham Young University.
- Ren, N., Wang, Y., Vilfayeau, S., & Trouvé, A. (2013). Large Eddy Simulation of Turbulent Vertical Wall Fires. 7th International Seminar on Fire and Explosion Hazards,
- Sharples, J. J., Edgar, R., & Sidhu, H. S. (2018). Investigation of slope thresholds for flame attachment. *Parte: <http://hdl.handle.net/10316.2/44517>*.
- Sullivan, A. L., Sharples, J. J., Matthews, S., & Plucinski, M. P. (2014). A downslope fire spread correction factor based on landscape-scale fire behaviour. *Environmental modelling & software*, 62, 153-163.
- Verma, S. (2019). *A large eddy simulation study of the effects of wind and slope on the structure of a turbulent line fire* University of Maryland, College Park].
- Wang, Y., Chatterjee, P., & de Ris, J. L. (2011). Large eddy simulation of fire plumes. *Proceedings of the Combustion Institute*, 33(2), 2473-2480.
- Weise, D. R., & Wright, C. S. (2014). Wildland fire emissions, carbon and climate: Characterizing wildland fuels. *Forest Ecology and Management*, 317, 26-40.
- Yang, H., Yan, R., Chen, H., Lee, D. H., & Zheng, C. (2007). Characteristics of hemicellulose, cellulose and lignin pyrolysis. *Fuel*, 86(12-13), 1781-1788.
- Yashwanth, B., Shotorban, B., Mahalingam, S., Lautenberger, C., & Weise, D. (2016). A numerical investigation of the influence of radiation and moisture content on pyrolysis and ignition of a leaf-like fuel element. *Combustion and flame*, 163, 301-316.
- Yashwanth, B., Shotorban, B., Mahalingam, S., & Weise, D. (2014). A numerical investigation of the effect of moisture content on pyrolysis and combustion of live fuels.